Neurochemical Research (2020) 45:2691–2702
https://doi.org/10.1007/s11064-020-03112-0

ORIGINAL PAPER

CircDHDDS/miR-361-3p/WNT3A Axis Promotes the Development of Retinoblastoma by Regulating Proliferation, Cell Cycle, Migration, and Invasion of Retinoblastoma Cells

Hongjun Wang[1] · Mingze Li[2] · Haibin Cui[3] · Xiangyuan Song[2] · Qian Sha[2]

Received: 3 January 2020 / Revised: 9 August 2020 / Accepted: 13 August 2020 / Published online: 31 August 2020

Abstract

Retinoblastoma (RB) is a common intraocular malignant tumor. The growing evidence has reported that circular RNAs (circRNAs) play critical roles in RB development. Therefore, the purpose of the study is to investigate the regulatory mechanism of circDHDDS in RB. The real-time quantitative polymerase chain reaction (RT-qPCR) assay was used to quantify the expression levels of circDHDDS, miR-361-3p, and WNT3A in RB tissues and cells (RPCs, Y-79, and WERI-Rb-1). The proliferation and cell cycle of RB cells were assessed by colony formation assay and flow cytometry assays, respectively. The migration and invasion of RB cells were measured by transwell assay. The protein expression levels of Nectin-3 (CD113), SOX2, Nanog, and WNT3A were measured by Western blot assay. The functional targets of circDHDDS and miR-361-3p were predicted by bioinformatics databases, and the dual-luciferase reporter assay was used to confirm the interaction relationship between miR-361-3p and circDHDDS or WNT3A. The functional role of circDHDDS silencing in vivo was evaluated by xenograft experiment. We found that circDHDDS was overexpressed in RB tissues and cells compared with normal retinas tissues and retinal pigment epithelial cells, correspondingly. Furthermore, silencing of circDHDDS impeded proliferation, migration, invasion, and induced cell cycle arrest in vitro, which were abolished by knockdown of miR-361-3p. The in vivo experiments also suggested that tumor growth was inhibited by knockdown of circDHDDS. Moreover, we also found that miR-361-3p specifically bound to WNT3A, and overexpression of miR-361-3p suppressed RB development by decreasing WNT3A expression. Summarily, circDHDDS, a molecule sponge of miR-361-3p, regulated the expression of WNT3A. Therefore, circDHDDS/miR-361-3p/WNT3A axis stimulated the development of RB by regulation of proliferation, cell cycle program, migration, and invasion of RB cells.

Keywords Circular RNA · circDHDDS · miR-361-3p · WNT3A · RB

Abbreviations

RB	Retinoblastoma
circRNA	Circular RNA
RT-qPCR	Real-time quantitative polymerase chain reaction

Introduction

Retinoblastoma (RB), originating from infants' retinal immature cells, is a rare malignant tumor of the retina [1]. According to the report, mortality of 9% can be reduced by efficient management of RB patients [2], thus early diagnosis and effective therapeutic methods for RB are quite critical [3, 4]. Therefore, it is required to develop new and reliable treatment methods for RB patients.

Circular RNAs (circRNAs) are a series of closed loop-form RNA molecules without 5′cap and a 3′poly A tail, characterized by abundance, stability, widely regulating multiple biological activities such as proliferation, apoptosis, and metastasis [5–7]. CircDHDDS (hsa_circ_0000034) is derived from the dehydrodolichol diphosphate synthase (DHDDS) gene and located on chr1 (26772806–26774151). Recently, Lyu et al. revealed that circDHDDS was

✉ Qian Sha
qpm8v5@163.com

[1] Department of Medical Administration, Shanghai Pudong Hospital, Shanghai, China

[2] Department of Ophthalmology, Shanghai Pudong Hospital, Shanghai, China

[3] Department of Ophthalmology, Heilongjiang Eye Hospital, Harbin, Heilongjiang, China

overexpressed in RB tissues when compared with corresponding normal retinal tissues [8]. Nevertheless, there are few reports regarding the regulatory mechanism of circDHDDS in RB.

MicroRNAs (miRNAs), 20–25 nucleotides in length, are a sort of RNAs without coding capacities [9]. It had been reported that miRNAs could act as regulator of gene expression by targeting the 3′untranslated region (3′UTR) of target mRNAs [10]. For instance, the upregulation of miR-361-3p could inhibit growth, migration and invasion of tumor cells in lung cancer [11]. Not surprisingly, miR-361-3p was reported to be an advantageous prognostic factor for cervical cancer patients [12]. Interestingly, Zhao et al. proposed that miR-361-3p was clearly decreased in tissues, serum, and cells of RB when compared with corresponding control groups [13]. Therefore, the potential mechanism of miR-382-5p need to be investigated in RB.

Furthermore, a recent research has discovered that Wnt/β-catenin pathway was highly connected with the progression of human cancer, including RB [14, 15]. WNT3A has been recognized as an important component of the Wnt/β-catenin signaling pathway, which was involved in cell proliferation, differentiation, and tumorigenesis [16, 17]. Mechanistically, Zhang et al. revealed that WNT3A activated Wnt/β-catenin signaling by enhancing β-catenin-dependent transcription [18].

Based on above studies and bioinformatics analysis, we hypothesized that circDHDDS could target miR-361-3p to regulate WNT3A expression in RB cells. In this study, we investigated the contributions of the circDHDDS on proliferation, migration, invasion, cell cycle progression of RB cells with a specific focus on its interactions with miR-361-3p and WNT3A.

Materials and Methods

Patient Specimens

We collected specimens of RB (n = 15) and normal retinas tissues (n = 10) from patients and volunteers, respectively, who underwent the surgical procedure at Shanghai Pudong Hospital between December 2014 and June 2018. The information of recruited patients was summarized in Table 1, and information of volunteers was presented in Table 2. All samples were frozen in snap-frozen and then transferred to a − 80 °C refrigerator. This study was ratified by the Ethics Committee of Shanghai Pudong Hospital with the approval No. 201411024, and performed in the light of the tenets of the Helsinki declaration as well as its later amendments. The written informed consents were provided by all patients and volunteers.

Table 1 The clinical characteristics of patients with RB

Case	Gender	Age (months)	Unilateral tumor	Bi-lateral tumor
1	Male	23	Yes	No
2	Male	20	Yes	No
3	Female	18	No	Yes
4	Male	10	No	No
5	Female	15	Yes	No
6	Female	9	No	Yes
7	Male	12	Yes	No
8	Male	14	No	Yes
9	Female	19	No	Yes
10	Female	20	Yes	No
11	Female	11	No	Yes
12	Male	17	No	Yes
13	Female	21	No	No
14	Male	8	Yes	No
15	Female	13	No	Yes

Table 2 The clinical characteristics of volunteers

Case	Gender	Age (months)	Unilateral tumor	Bi-lateral tumor
1	Female	12	No	No
2	Male	19	No	No
3	Male	20	No	No
4	Female	17	No	No
5	Male	15	No	No
6	Female	10	No	No
7	Male	23	No	No
8	Male	18	No	No
9	Female	19	No	No
10	Female	15	No	No

Cell Lines and Cell Culture

RB cells (Y-79 and WERI-Rb-1) were obtained from the American Type Culture Collection (Rockville, MD, USA). Retinal progenitor cells (RPCs) were purchased from BeNa Culture Collection (Beijing, China). These cells were propagated in RPMI-1640 medium plus 10% (v/v) fetal bovine serum (Biochrom, Berlin, Germany) and 1% penicillin/streptomycin (Biochrom) in a humidified atmosphere containing 5% CO_2 at 37 °C.

Real-Time Quantitative Polymerase Chain Reaction (RT-qPCR)

Total RNA was isolated using Trizol reagent (Life Technologies Corporation, Carlsbad, CA, USA) based on the recommendations. Concentration and purity of RNA were assessed under a Nanodrop 2000c (Thermo Fisher Scientific, Carlsbad, CA, USA). Subsequently, RNA was switched to complementary DNA using reverse transcription kit (Takara, Dalian, China) or New Poly (A) Tailing microRNA Reverse Transcription Kit (Thermo Fisher Scientific). RT-qPCR analysis was conducted to quantitatively analyze the expression levels of RNA based on the $2^{-\Delta\Delta Ct}$ method. The glyceraldehyde-3-phosphate dehydrogenase (GAPDH) and small nuclear RNA U6 were served as a reference control. For RNase R treatments assay, 20 μg of RNA was treated with RNase R (Epicenter Biotechnologies, Madison, WI, USA) at 37 °C for 15 min. In addition, cytoplasmic and nuclear fractions were isolated using NE-PER Reagent (Thermo Fisher Scientific) in line with the instructions of manufacturer.

The primers were shown as follow:

circDHDDS (F-5′-ATGCTGTGAGAGAGATGGCCT-3′; R-5′-AGGGCAACAAGTGCAGATCG-3′);

DHDDS (F-5′-TGCCGAAACACATTGCATTCA-3′; R-5′-GCGTAGACTGTCACCTCTAGGAT-3′);

miR-361-3p (F-5′-GCCGAGTCCCCCAGGTGTGATT-3′; R-5′-CTCAACTGGTGTCGTGGA-3′);

WNT3A (F-5′-CTCCTCTCGGATACCTCTTAGTG-3′; R-5′-CCAAGGACCACCAGATCGG-3′);

GAPDH (F-5′-TCCCATCACCATCTTCCAGG-3′; R-5′-GATGACCCTTTTGGCTCCC-3′);

U6 (F-5′-AACGCTTCACGAATTTGCGT-3′; R-5′- CTC GCTTCGGCAGCACA-3′).

Transfection Assay

Small interfering RNA (siRNA) against circDHDDS (si-circDHDDS) and siRNA scrambled control (si-NC) were purchased from GenePharma (Shanghai, China). The sequence for si-circDHDDS sense: 5′-UGCAAAACAGAC AUUCAGGAA-3′; antisense, 5′-CCUGAAUGUCUGUUU UGCAUA-3′. The sequence for siRNA sense: 5′-GGCCUA AAGUAGUAGCUAUTT-3′; antisense, 5′-AUAGCUACU ACU UUAGGCCTT-3′. MiR-361-3p mimic (miR-361-3p) and its negative control (miR-NC), and miR-361-3p inhibitor (anti-miR-361-3p) and its negative control (anti-miR-NC) were designed by GenePharma. WNT3A-overexpression vector (WNT3A) and its negative control (vector), and short hairpin RNA (sh-RNA) targeting circDHDDS (sh-circDHDDS) and its negative control (sh-NC) were constructed by Biossci Company (Wuhan, China). RB cells were seeded into 6-well plates and cultured overnight. The above siRNA, mimic, inhibitor, vector or sh-RNA was transfected into Y-79 and WERI-Rb-1 cells by Lipofectamine® 2000 (Thermo Fisher Scientific) referring to the producer's procedures.

Colony Formation Assay

The colony formation assay with soft agar was performed as described by Ni et al. [19]. Briefly, Y-79 and WERI-Rb-1 cells were seeded into 12-well plate at a density of 500 cells/well, with un-transfected cells as control. After culturing for 14 days, the 12-well plate were washed with phosphate buffered saline. After that, the colonies were fixed by 95% ethanol for 5 min and then dyed by 0.1% crystal violet for 10 min. The colonies were calculated under the microscope (Olympus, Tokyo, Japan).

Flow Cytometry Analysis

For cell cycle evaluation, transfected cells or control cells were collected at 48 h post-transfection and then fixed by 75% ethanol overnight at 4 °C. After that, cells were incubated with RNase A and stained with propidium iodide (PI; Sigma, St. Louis, MO, USA) at room temperature in the dark condition for 15 min. Cell cycle was examined under the FACScan flow cytometer (BD Biosciences, San Jose, CA, USA), and the percentages of cells in various mitotic phases was analyzed under the ModFit software (BD Biosciences).

Transwell Assay

The transwell migration assay was performed using the 24-well transwell chamber (8-μm pore size; Corning Inc, Corning, NY, USA). In brief, 1×10^5 RB cells in 200 μL of serum-free medium were seeded into the upper chambers. While 600 μL of RPMI-1640 medium contained with 10% serum was added into low chambers. After incubation for 24 h, the RB cells on the upper chambers were lightly removed, while migratory cells were fixed by 95% ethanol for 30 min and dyed by crystal violet. Finally, the numbers of the migrated cells were calculated in five randomly chosen fields under the inverted microscope (Olympus). Notably, the upper chambers of transwell chambers were pre-adhered with Matrigel (BD Biosciences) for invasion analysis, while other steps were consistence with migration assay.

Western Blot Assay

Briefly, the protein from tissue samples and cells was isolated using RIPA Lysis Buffer (catalogue number: 20-188; Millipore, Bedford, MA, USA). The density of protein was examined by Bicinchoninic Acid Kit (Thermo Fisher Scientific). After that, 40 μg of total protein was electrophoretically transferred onto polyvinylidene fluoride membranes (Millipore) after separating by 10% sodium dodecyl sulfate

polyacrylamide gel electrophoresis. The 5% skim milk solution was applied to block the membranes for 1 h at room temperature. After blocking for nonspecific binding, the membranes were incubated with antibody overnight: anti-Nectin-3 (CD113; ab63931; 1:1000 dilution; Abcam, Cambridge, MA, USA), anti-SOX2 (ab97959; 1:1000 dilution; Abcam), anti-Nanog (ab109250; 1:1000 dilution; Abcam), anti-WNT3A (ab219412; 1:1000 dilution; Abcam), or anti-GAPDH (ab181602; 1:1000 dilution; Abcam). Subsequently, the membranes were reacted to the horseradish peroxidase-conjugated secondary antibody (ab150077, 1:3000 dilution, Abcam). Eventually, the antibody binding was captured by using Clarity™ Western ECL Substrate Kit (Bio-Rad, Hercules, CA, USA). The signal intensity was measured by using Image Lab™ Software (Bio-Rad).

Dual-Luciferase Reporter Assay

The binding sites of miR-361-3p in circDHDDS or 3′UTR of WNT3A were predicted using the bioinformatics databases Starbase v2.0 (https://starbase.sysu.edu.cn/) or Targetscan (https://www.targetscan.org/mamm_31/), respectively. RB cells were co-transfected with miR-361-3p or miR-NC and pGL3 Luciferase Reporter Vectors (Promega, Madison, WI, USA) containing circDHDDS WT, circDHDDS MUT, WNT3A 3′UTR WT, or WNT3A 3′UTR MUT according to experimental design. After transfection 48 h, luciferase activity in RB cells was detected by the dual-luciferase reporter assay system (Promega) referring to the manufacturer's procedures.

In Vivo Experiment

Y-79 and WERI-Rb-1 cells were stably transfected with lentiviral vectors contained with sh-circDHDDS or sh-NC. In briefly, 24 BALB/c nude mice (4 weeks; National Laboratory Animal Center, Beijing, China) were divided into four groups (n = 6) and fed in pathogen-free environment. A total of 1×10^7 RB cells were hypodermically injected into the dorsal right flank of BALB/c nude mice. Tumor size was calculated every 5 days with the formula $V = 1/2 \times ab^2$ method (length (a) and width (b) length of the tumor). After 30 days, mice were euthanized, and the tumor tissues were harvested for the weight detection and total RNA or protein extraction. Animal experiments were supported and permitted by the Institutional Animal Care and Use Committee of Shanghai Pudong Hospital.

Statistical Analysis

All data were analyzed using SPSS 21.0 software (IBM, Somers, NY, USA), and P-value < 0.05 was regarded as significant difference. Differences between two groups or multiple groups were evaluated using the Student's t-test or one-way analysis of variance, respectively. The results were exhibited as the mean ± standard deviation from three independent experiments.

Results

CircDHDDS was Overexpressed in RB Tissues and Cells

Initially, we compared circDHDDS expression in RB tissues and normal retinas tissues using RT-qPCR analysis. As presented in Fig. 1a, circDHDDS was increased in RB tissues when compared with control. Likewise, the results of RT-qPCR analysis implied that circDHDDS was overexpressed in RB compared with RPCs cells (Fig. 1b). Given of circRNA could resist RNase R degradation because of without 5′cap and a 3′poly A tail. Next, total RNA was treated with RNase R for RT-qPCR assay and results suggested that circDHDDS was more resistant to RNase R than linear DHDDS mRNA (Fig. 1c, d). In addition, the results of RT-qPCR analysis revealed that circDHDDS was mainly located in the cytoplasm (Fig. 1e, f). Considering circDHDDS was increased in RB tissues and cells, the role of circDHDDS in RB was investigated in the next experiment.

Knockdown of circDHDDS Inhibited Proliferation, Migration, and Invasion and Cell Cycle Program in RB Cells

To investigate the role of circDHDDS in RB cells, we knocked down the expression of circDHDDS in Y-79 and WERI-Rb-1 cells using si-circDHDDS in subsequence experiments. As shown in Fig. 2a, b, circDHDDS was obviously downregulated in RB cells transfected with si-circDHDDS compared with these cells transfected with si-NC. Moreover, proliferation capability of Y-79 and WERI-Rb-1 cells was inhibited by knockdown of circDHDDS (Fig. 2c). Inhibition of circDHDDS induced cell cycle arrest at G0/G1 phase and decreased S and G2/M phases-cells (Fig. 2d, e). The results of transwell assay implied that migration and invasion were repressed in Y-79 and WERI-Rb-1 cells after silencing of circDHDDS (Fig. 2f, g). The effects of circDHDDS silencing on RB cell stemness were assessed by measuring the expression of stem cell markers, including CD133, SOX2 and Nanog by Western blot analysis, and the results indicated that CD133, SOX2, and Nanog were all declined in si-circDHDDS group compared with si-NC group (Fig. 2h, i). Altogether, these data showed that suppression of circDHDDS inhibited proliferation, migration, and invasion and induced cell cycle arrest in RB cells.

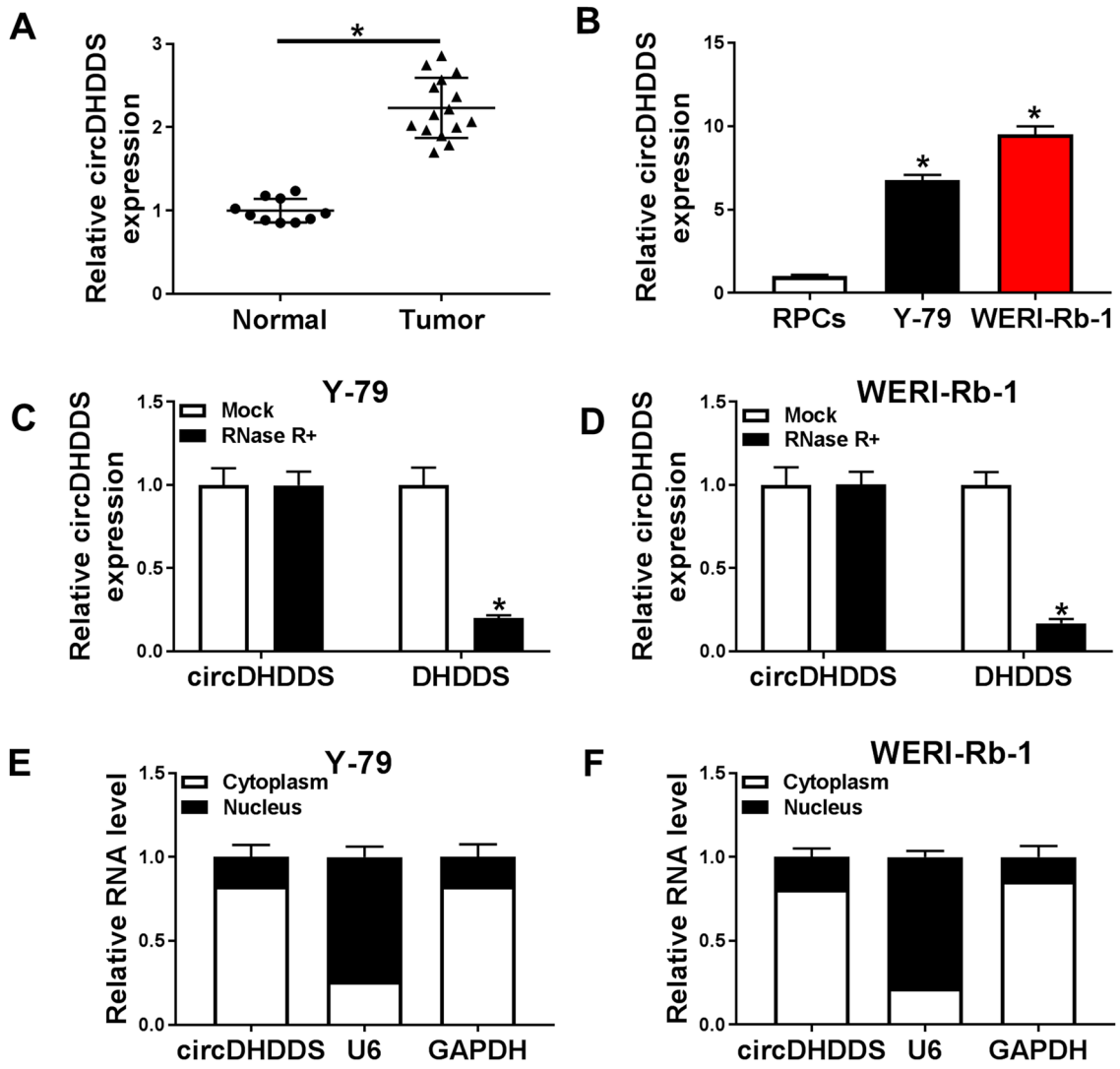

Fig. 1 The expression level of circDHDDS in retinoblastoma tissues and cells. **a**, **b** The relative expression level of circDHDDS was measured by RT-qPCR assay in retinoblastoma tissues and cells, as well as in matched controls. **c**, **d** Following RNase R treatment, the expression level of circDHDDS and DHDDS was analyzed by RT-qPCR analysis in Y-79 and WERI-Rb-1 cells. **e**, **f** The expression levels of circDHDDS, U6, and GAPDH in cytoplasm and nucleus were shown by RT-qPCR assay. All data exhibited as the mean ± standard deviation from three independent experiments. $^{*}P < 0.05$

CircDHDDS Negatively Regulated miR-361-3p Expression in RB Cells

To identify the targets of circDHDDS, we initially used bioinformatics database analysis, and the predicted results indicated that circDHDDS had binding sequences in miR-361-3p, as presented in Fig. 3a. Subsequently, we also observed that luciferase activity of circDHDDS WT group was decreased by overexpression of miR-361-3p when compared with miR-NC group, while luciferase activity of circDHDDS MUT was not changed by miR-361-3p mimic (Fig. 3b, c). Furthermore, we also found that miR-361-3p was upregulated in Y-79 and WERI-Rb-1 cells after knockdown of circDHDDS, implying that miR-361-3p was negatively regulated by circDHDDS in RB cells (Fig. 3d, e). Interestingly, miR-361-3p was downregulated in RB tissues and cells compared with respective controls (Fig. 3f, g). Eventually, miR-361-3p was negatively corrected with circDHDDS expression in RB tissues (Fig. 3h). Conclusively, miR-361-3p was a functional target of circDHDDS in RB cells.

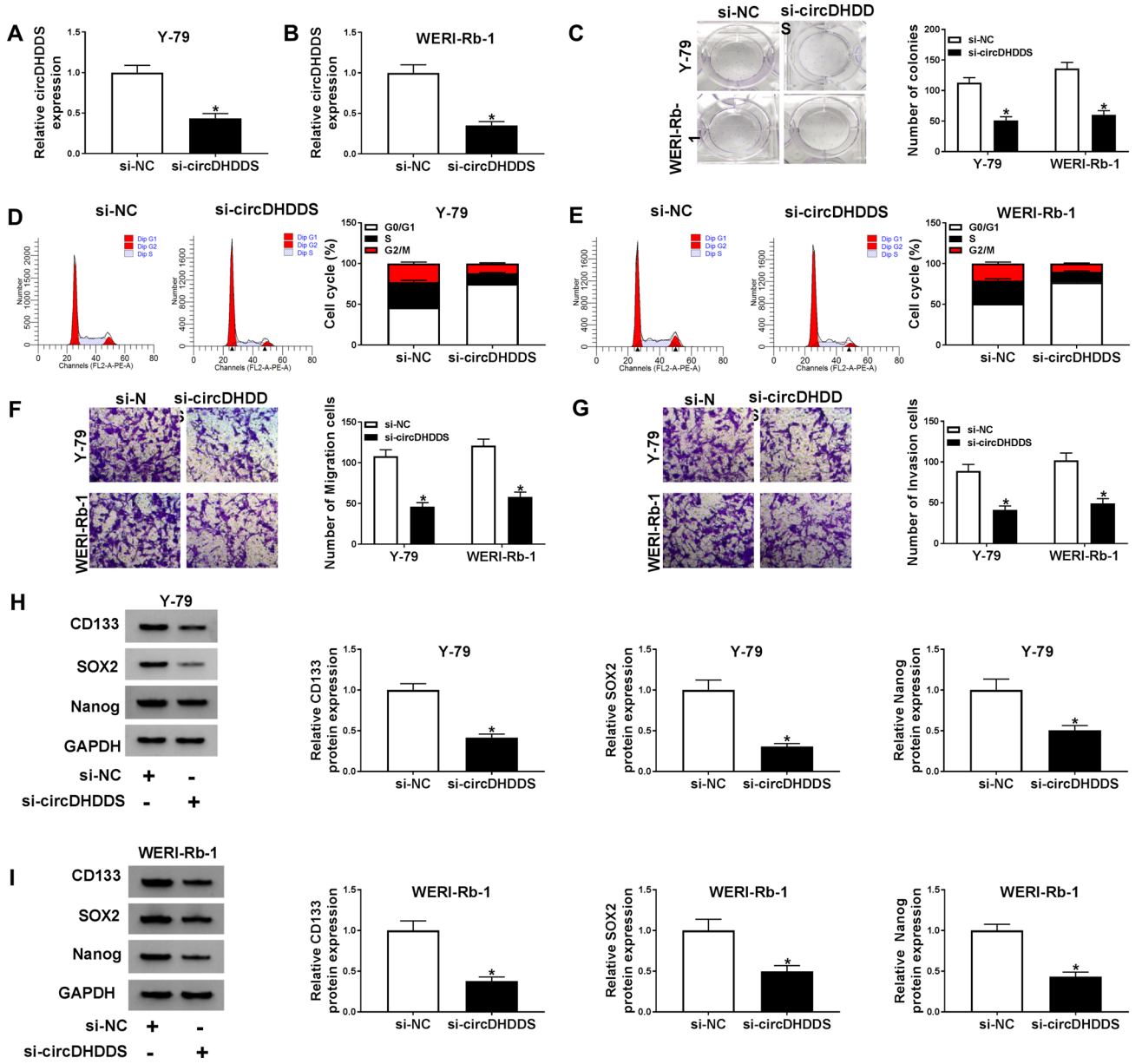

Fig. 2 The influences of circDHDDS knockdown on proliferation, cell cycle distribution, migration, and invasion of retinoblastoma cells. **a**, **i** Y-79 and WERI-Rb-1 cells were transfected with si-NC or si-circDHDDS. **a**, **b** The RT-qPCR analysis was used to examine circDHDDS level in Y-79 and WERI-Rb-1 cells at post-transfection. **c** The proliferation ability of Y-79 and WERI-Rb-1 cells was measured by colony formation assay. **d**, **e** Cell cycle distribution of Y-79 and WERI-Rb-1 cells was presented by flow cytometry analysis. **f**, **g** Transwell migration and invasion assays were employed to measure the migration and invasion abilities of Y-79 and WERI-Rb-1 cells. **h**, **i** Western blot analysis was carried out to show CD133, SOX2, and Nanog levels in Y-79 and WERI-Rb-1 cells. All data exhibited as the mean ± standard deviation from three independent experiments. $^{*}P < 0.05$

CircDHDDS Regulated Proliferation, Cell Cycle Process, Migration, and Invasion of RB Cells by Targeting miR-361-3p

Since miR-361-3p was a functional target of circDHDDS, the association between miR-361-3p and circDHDDS was further investigated. As displayed in Fig. 4a, b, knockdown of miR-361-3p could weaken the suppressive effect on miR-361-3p expression in Y-79 and WERI-Rb-1 cells induced by si-circDHDDS. Co-transfection of miR-361-3p inhibitor and si-circDHDDS into Y-79 and WERI-Rb-1 cells could abate the inhibitory effect on cell proliferation induced by transfection with si-circDHDDS along (Fig. 4c, d). Moreover, knockdown of circDHDDS induced cell cycle arrest, which was overturned by downregulation of miR-361-3p expression in

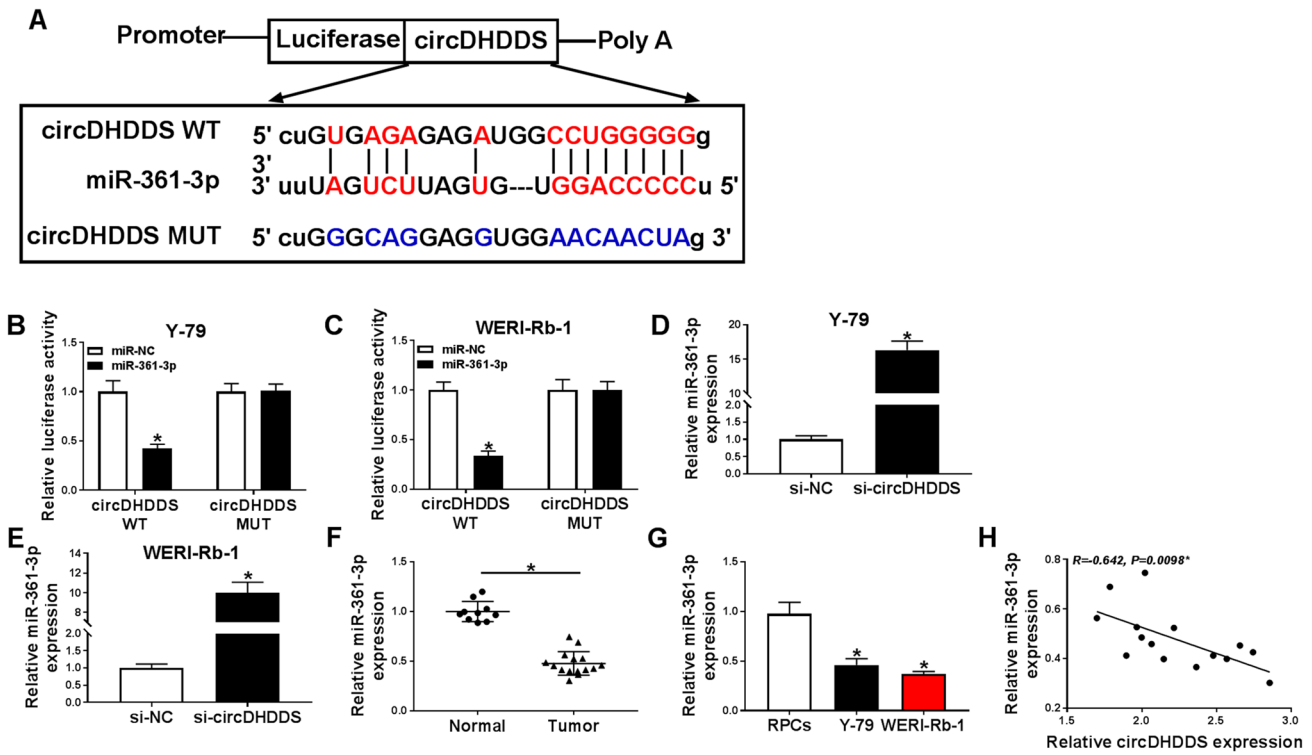

Fig. 3 MiR-361-3p was a functional target of circDHDDS in retinoblastoma cells. **a** The putative binding sequences of miR-361-3p in circDHDDS, and matched mutant sites were shown. **b**, **c** The luciferase activity was measured in Y-79 and WERI-Rb-1 cells by performing dual-luciferase report assay. **d**, **e** RT-qPCR assay was conducted to evaluate the expression level of miR-361-3p in Y-79 and WERI-Rb-1 cells transfected with si-NC or si-circDHDDS. **f**, **g** The expression level of miR-361-3p was assessed by RT-qPCR assay in retinoblastoma tissues and normal retinas tissues, along with in RPCs, Y-79 and WERI-Rb-1 cells. **h** The relationship between circDHDDS and miR-361-3p was analyzed by Pearson's correlation analysis. All data exhibited as the mean ± standard deviation from three independent experiments. $^{*}P < 0.05$

Y-79 and WERI-Rb-1 cells (Fig. 4e, f). The results of transwell analysis indicated that inhibition of miR-361-3p was able to partly rescue the loss of the migration and invasion abilities in Y-79 and WERI-Rb-1 cells caused by circDHDDS knockdown (Fig. 4g, h). Additionally, Western blot assay suggested that knockdown of circDHDDS inhibited the expression of CD133, SOX2, and Nanog, whereas these effects were abolished by suppression of miR-361-3p in Y-79 and WERI-Rb-1 cells (Fig. 4i, j). Therefore, knockdown of circDHDDS impeded proliferation, migration, and invasion, and arrested cell cycle process in RB cells by targeting miR-361-3p.

WNT3A Acted as a Direct Target of miR-361-3p in RB Cells

We investigated the involvement of target mRNA of miR-361-3p in RB cells using bioinformatics software. As shown in Fig. 5a, miR-361-3p has the complementary base pairing in 3′UTR of WNT3A mRNA. We noticed that miR-361-3p mimic significantly decreased the luciferase activity of WNT3A 3′UTR WT, while had no effect on luciferase activity of WNT3A 3′UTR MUT compared with control group (Fig. 5b, c). The expression level of WNT3A was suppressed in Y-79 and WERI-Rb-1 cells after transfection with miR-361-3p, no matter mRNA or protein (Fig. 5d, e). More importantly, downregulation of miR-361-3p could rescue si-circDHDDS-mediated downregulation of WNT3A expression in Y-79 and WERI-Rb-1 cells (Fig. 5f, g). The RT-qPCR and Western blot assays confirmed that WNT3A was overexpressed in RB tissues and cells when compared with matched controls (Fig. 5h–k). Additionally, WNT3A was inversely correlated with miR-361-3p while positively correlated with circDHDDS expression in RB tissues (Fig. 5l, m). All results implied that circDHDDS regulated WNT3A expression by targeting miR-361-3p in RB cells.

Restoration of WNT3A Reversed the Tumor-Inhibitor Roles of miR-361-3p in RB Cells

The association between WNT3A and miR-361-3p was investigated in next experiments. We found that transfection with WNT3A significantly increased WNT3A expression that was inhibited by miR-361-3p mimic (Fig. 6a, b).

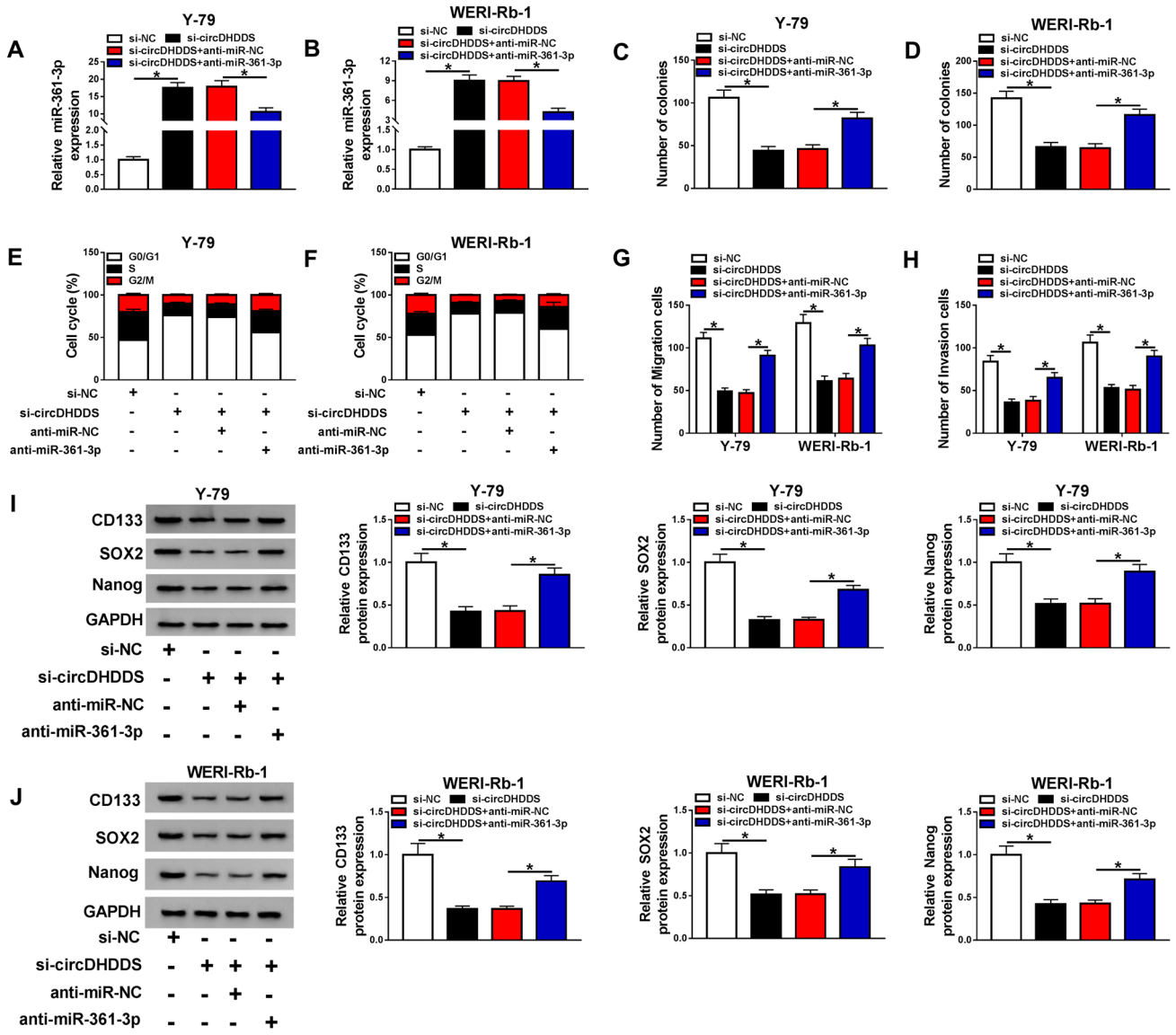

Fig. 4 CircDHDDS regulated proliferation, cell cycle, migration, and invasion of retinoblastoma cells by targeting miR-361-3p. **a**–**j** Y-79 and WERI-Rb-1 cells were transfected with si-NC, si-circDHDDS, si-circDHDDS+anti-miR-NC, or si-circDHDDS+anti-miR-361-3p. **a**, **b** RT-qPCR was used to measure expression level of miR-361-3p in Y-79 and WERI-Rb-1 cells. **c**, **d** The colony formation assay was conducted for measuring the cell proliferation of Y-79 and WERI-Rb-1. **e**, **f** Flow cytometry analysis was used to assess cell cycle distribution in Y-79 and WERI-Rb-1 cells after transfection. **g**, **h** Cell migration and invasion assays were performed in transfected Y-79 and WERI-Rb-1 cells. **i**, **j** The protein expression levels of CD133, SOX2, and Nanog were determined by Western blot assay in Y-79 and WERI-Rb-1 cells. All data exhibited as the mean ± standard deviation from three independent experiments. $^{*}P < 0.05$

Additionally, colony formation assay manifested that the suppressive effect on cell proliferation caused by miR-361-3p was recovered by overexpression of WNT3A in Y-79 and WERI-Rb-1 cells (Fig. 6c). The results of flow cytometry suggested that overexpression of WNT3A abolished miR-361-3p-induced cell cycle arrest (Fig. 6d, e). The upregulation of miR-361-3p inhibited cell migration and invasion, while these effects could be abolished by restoration expression of WNT3A in Y-79 and WERI-Rb-1 cells (Fig. 6f, g). Moreover, the results of Western blot assay revealed that the downregulation of CD133, SOX2, and Nanog induced by miR-361-3p mimic was rescued by overexpression of WNT3A in Y-79 and WERI-Rb-1 cells (Fig. 6h, i). Therefore, miR-361-3p might act as a tumor suppressor in RB cells, which was involved WNT3A.

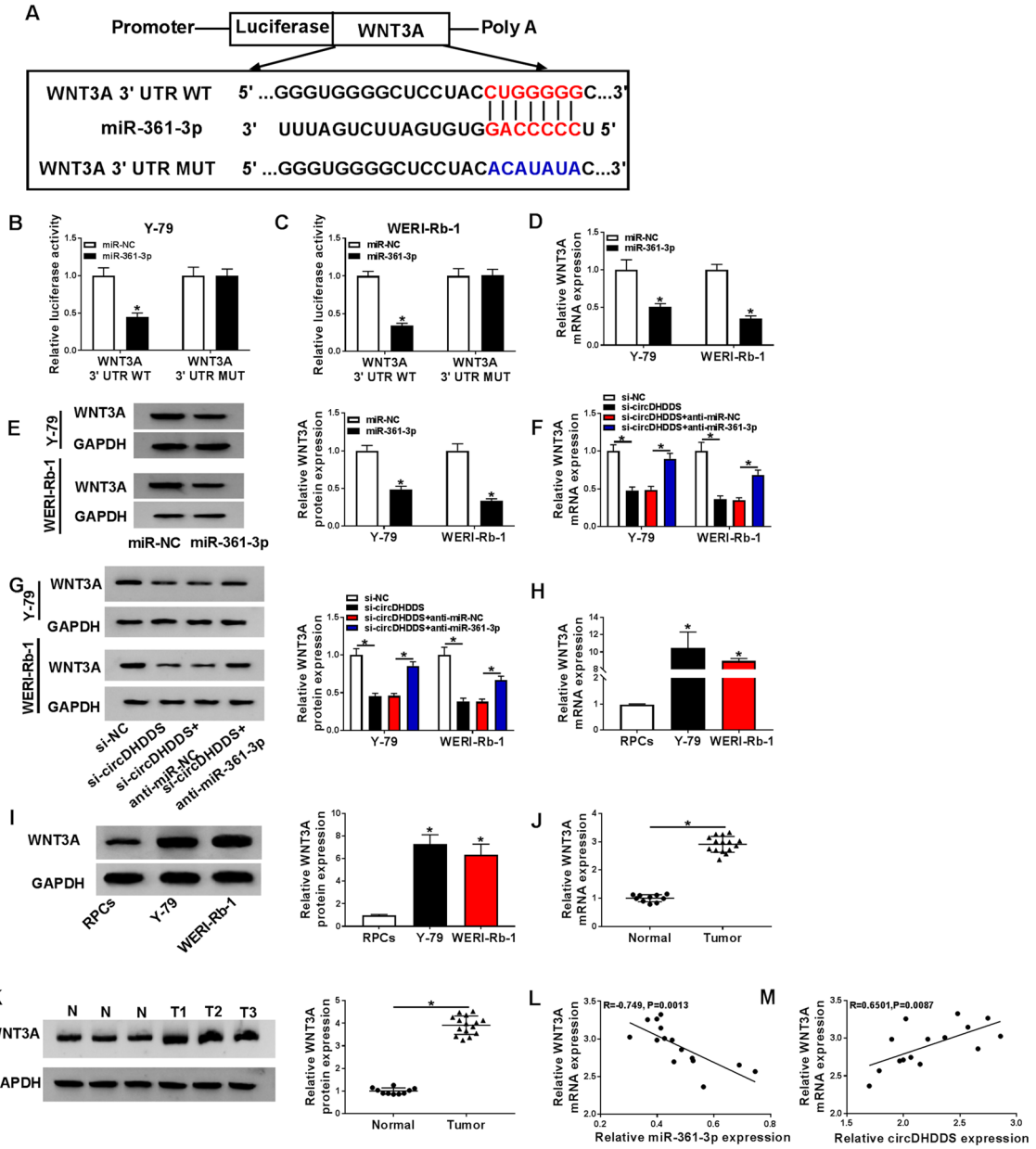

Fig. 5 CircDHDDS regulated WNT3A expression by targeting miR-361-3p. **a** Binding region between miR-361-3p and 3′UTR of WNT3A were shown. **b**, **c** Dual-luciferase reporter assay was used to prove interaction relationship between miR-361-3p and 3′UTR of WNT3A mRNA in Y-79 and WERI-Rb-1 cells. **d**, **e** The expression levels of WNT3A were examined by RT-qPCR and Western blot assays in Y-79 and WERI-Rb-1 cells transfected with miR-361-3p or miR-NC. **f**, **g** The mRNA and protein expression level of WNT3A were evaluated by RT-qPCR and Western blot assays in Y-79 and WERI-Rb-1 cells transfected with si-NC, si-circDHDDS, si-circDHDDS+anti-miR-NC, or si-circDHDDS+anti-miR-361-3p. **h**–**k** The RT-qPCR and Western blot analyses were carried out to examine the expression of WNT3A in retinoblastoma tissues and cells, along with in matched negative controls. **l**, **m** The correction relationship between WNT3A and miR-361-3p or circDHDDS was analyzed in retinoblastoma tissues. All data exhibited as the mean ± standard deviation from three independent experiments. $^{*}P < 0.05$

Inhibition of circDHDDS Repressed RB Tumor Growth In Vivo

Based on above results, silencing of circDHDDS inhibited proliferation of RB cells, the function of circDHDDS knockdown was investigated in vivo. As shown in Fig. 7a, the tumor tissues from sh-circDHDDS group had lower growth rate compared with tumor tissues from sh-NC group. Consistently, knockdown of circDHDDS also decreased tumor weight compared with sh-NC group (Fig. 7b). In

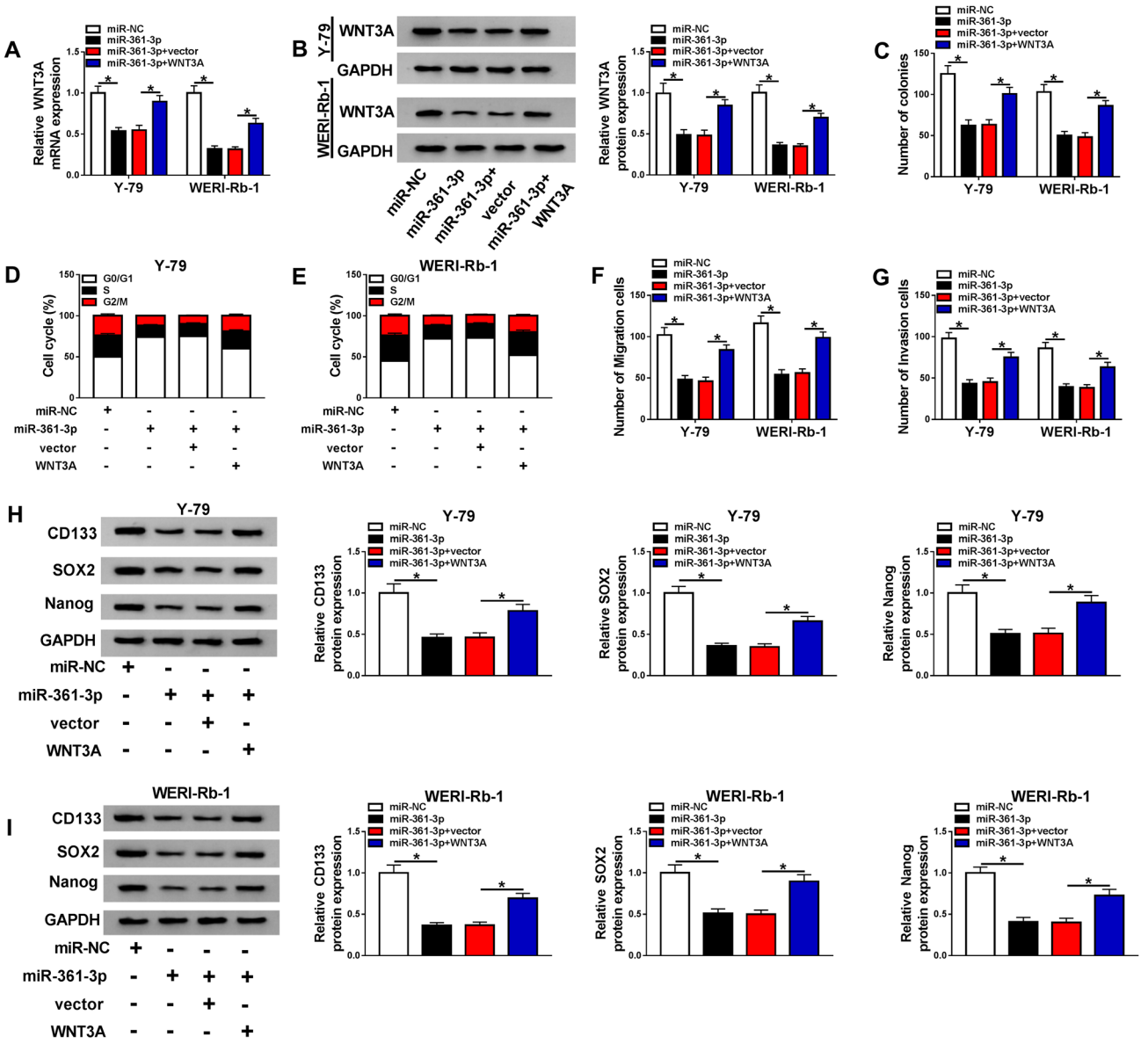

Fig. 6 Overexpression of WNT3A reversed miR-361-3p-induced the effects on proliferation, cell cycle distribution, migration, and invasion in retinoblastoma cells. **a**–**i** Y-79 and WERI-Rb-1 cells were transfected with miR-NC, miR-361-3p, miR-361-3p+vector, or miR-361-3p+WNT3A. **a**, **b** The expression levels of WNT3A were measured by RT-qPCR and Western blot assays in Y-79 and WERI-Rb-1 cells. **c** The colony formation assay was performed in Y-79 and WERI-Rb-1 post-transfection. **d**, **e** Cell cycle distribution of Y-79 and WERI-Rb-1 cells was measured by flow cytometry assay in each group. **f**, **g** The cell numbers of migration and invasion were displayed by transwell analysis in Y-79 and WERI-Rb-1 cells. **h**, **i** The protein levels of CD133, SOX2, and Nanog were analyzed by Western blot assay in Y-79 and WERI-Rb-1 cells. All data exhibited as the mean ± standard deviation from three independent experiments. $^{*}P < 0.05$

addition, circDHDDS was decreased while miR-361-3p was increased in sh-circDHDDS group when compared to sh-NC group (Fig. 7c). As demonstrated by Fig. 7d, e, the mRNA and protein expression levels of WNT3A were down-regulated in xenografts of sh-circDHDDS group compared with sh-NC group. In summary, these results indicated that suppression of circDHDDS decreased tumor growth in vivo.

Discussion

In this study, we found that RB tissues and cells showed higher level of circDHDDS when competed with negative groups. More importantly, the silencing of circDHDDS restrained cell growth, migration and invasion while facilitated cell cycle arrest at G0/G1 in RB cells. In addition, inhibition of circDHDDS also reduced cancer stem cell

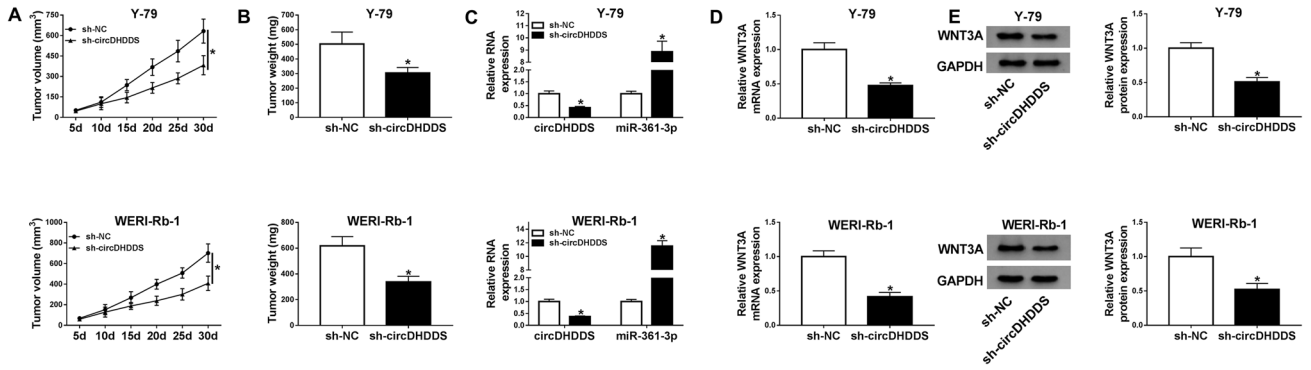

Fig. 7 Effects of circDHDDS silencing on retinoblastoma tumor growth in vivo. **a**, **b** The growth curves and weight of retinoblastoma tumors were shown. **c**, **d** The expression levels of circDHDDS, miR-361-3p and WNT3A in tumor samples were examined with RT-qPCR assay. **e** The protein expression level of WNT3A was assessed by Western blot assay. All data exhibited as the mean ± standard deviation from three independent experiments. $^{*}P < 0.05$

properties, decreasing CD133, SOX2, and Nanog expression in RB cells. It is a critical issue in the field of targeting cancer stem cells for treatment resistance and relapse of human cancers [20].

It had been widely proposed that circRNAs could act as miRNA sponges to participate in transcriptional and post-transcriptional regulation of gene expression [21, 22]. In particular, circRNA could exert the miRNA sponge activity in the cytoplasm [23], and our results indicated the main cytoplasm distribution of circDHDDS, suggesting the possibility that circDHDDS acted as a miRNA sponge. However, the underlying mechanism of circDHDDS remained unknown in RB.

In addition, miRNAs play important roles in cell differentiation, tissue development, and the development of tumor [24]. The bioinformatics analysis identified that miR-361-3p was a novel target of circDHDDS. Consistent with a previous study [13], we also found a decreased expression of miR-361-3p in RB tumor tissues compared with control group. Several reports have demonstrated an association between miR-361-3p and malignancies, revealing that miR-361-3p was downregulated and acted as a tumor suppressor in many cancers [11–13]. Therefore, we speculated that miR-361-3p might target crucial oncogenes and play a role as tumor inhibitory miRNA in RB. Zhao and colleague reported that GLI1 and GLI3 were direct targets of miR-361-3p in RB [13]. It is possible that miR-361-3p regulates not only GLI1 and GLI3 but also other targets, which could be explained because of one miRNA can target multiple mRNAs [25]. The different target mRNAs of miR-361-3p was found in pancreatic ductal adenocarcinoma and human oral cancer [26, 27].

In this paper, WNT3A was predicted as a possible functional target of miR-361-3p. It had been reported that WNT3A was overexpressed in hepatocellular carcinoma and colon cancer [28, 29]. WNT3A is an important component of the Wnt/β-catenin signaling pathway [16, 17]. The overexpression of miR-15a-5p restrained proliferation and stemness of HEC-1-A cell by targeting WNT3A [30]. Analogously, the functional experiments confirmed that WNT3A was inhibited by miR-485 in RB cells to further inactivate Wnt/β-catenin pathway in RB cells [31]. Not surprisingly, WNT3A was one of the downstream target of miR-361-3p in RB. Nevertheless, the limitations were faced in this study. A limited sample size was used during the study, which may lead un-objective conclusion. Given that the expression level of WNT3A was shown to be associated with cell growth and drug-resistance in tumor cells through Wnt/β-catenin pathway [32, 33], while we not clarify relationship between circDHDDS/miR-361-3p/WNT3A axis and Wnt/β-catenin pathway in RB. Furthermore, although we revealed the some functions of circDHDDS, the multivariate analysis with cox analysis should be performed to verify the diagnostic value of circDHDDS for RB patients.

In summary, circDHDDS acted as an oncogene and promoted RB development by regulating proliferation, migration, invasion, and cell cycle progression by targeting miR-361-3p/WNT3A axis in RB, which may be a new perspective to the function of circDHDDS in RB.

Conclusion

Collectively, current findings implied that circDHDDS was upregulated in RB tissues and cells. The knockdown of circDHDDS inhibited RB cell growth, migration and invasion, and arrested cell cycle. Mechanistically, circDHDDS could directly interact with miR-361-3p, and subsequently functioned as a miR-361-3p sponge to regulate the expression of the WNT3A, which may enhance the development of RB. These results suggested that the contributions of the

circDHDDS in RB was attributed to its interactions with miR-361-3p and WNT3A partially.

Author contributions Conceptualization and Methodology: ML and HC; Formal analysis and Data curation: XS and QS; Validation and Investigation: HW and XS; Writing—original draft preparation and Writing—review and editing: HW, ML and HC; Approval of final manuscript: all authors.

Funding No funding was received.

Data Availability The analyzed data sets generated during the present study are available from the corresponding author on reasonable request.

Compliance with Ethical Standards

Conflict of interest The authors declare that they have no competing interests.

Ethical Approval The present study was approved by the ethical review committee of The Second Hospital of Hebei Medical University.

Informed Consent Written informed consent was obtained from all enrolled patients.

References

1. Kivelä TT, Hadjistilianou T (2017) Neonatal retinoblastoma. Asia Pac J Oncol Nurs 4:197–204
2. Ahmad A (2016) Retinoblastoma-clinical spectrum and treatment outcome in children. J Rawalpindi Med Coll 20:198–201
3. Gao J, Zeng J, Guo B, He W, Chen J, Lu F et al (2016) Clinical presentation and treatment outcome of retinoblastoma in children of South Western China. Medicine 95:e5204
4. Waddell KM, Kagame K, Ndamira A, Twinamasiko A, Picton SV, Simmons IG et al (2015) Clinical features and survival among children with retinoblastoma in Uganda. Br J Ophthalmol 99:387–390
5. Memczak S, Jens M, Elefsinioti A, Torti F, Krueger J, Rybak A et al (2013) Circular RNAs are a large class of animal RNAs with regulatory potency. Nature 495:333
6. Yu T, Wang Y, Fan Y, Fang N, Wang T, Xu T et al (2019) CircRNAs in cancer metabolism: a review. J Hematol Oncol 12:90
7. Zhu L-P, He Y-J, Hou J-C, Chen X, Zhou S-Y, Yang S-J et al (2017) The role of circRNAs in cancers. Biosci Rep 37:BSR20170750
8. Lyu J, Wang Y, Zheng Q, Hua P, Zhu X, Li J et al (2019) Reduction of circular RNA expression associated with human retinoblastoma. Exp Eye Res 184:278–285
9. Schirle NT, Sheu-Gruttadauria J, MacRae IJ (2014) Structural basis for microRNA targeting. Science 346(6209):608–613
10. Farazi TA, Spitzer JI, Morozov P, Tuschl T (2011) miRNAs in human cancer. J Pathol 223:102–115
11. Chen W, Wang J, Liu S, Wang S, Cheng Y, Zhou W et al (2016) MicroRNA-361-3p suppresses tumor cell proliferation and metastasis by directly targeting SH2B1 in NSCLC. J Exp Clin Cancer Res 35:76
12. Liu S, Song L, Yao H, Zhang L, Xu D, Li Q et al (2018) Preserved miR-361-3p expression is an independent prognostic indicator of favorable survival in cervical cancer. Dis Mark. https://doi.org/10.1155/2018/8949606
13. Zhao D, Cui Z (2019) MicroRNA-361-3p regulates retinoblastoma cell proliferation and stemness by targeting hedgehog signaling. Exp Ther Med 17:1154–1162
14. Dzobo K, Thomford NE, Senthebane DA (2019) Targeting the versatile Wnt/β-catenin pathway in cancer biology and therapeutics: from concept to actionable strategy. OMICS 23(11):517–538
15. Liao YJ, Yin XL, Deng Y (2019) Peng XW (2019) PRC1 gene silencing inhibits proliferation, invasion, and angiogenesis of retinoblastoma cells through the inhibition of the Wnt/β-catenin signaling pathway. J Cell Biochem 120(10):16840–16852
16. Yun M-S, Kim S-E, Jeon SH, Lee J-S, Choi K-Y (2005) Both ERK and Wnt/β-catenin pathways are involved in Wnt3a-induced proliferation. J Cell Sci 118:313–322
17. He S, Lu Y, Liu X, Huang X, Keller ET, Qian C-N et al (2015) Wnt3a: functions and implications in cancer. Chin J Cancer 34:50
18. Zhang S, Chen X, Hu Y, Wu J, Cao Q, Chen S et al (2016) All-trans retinoic acid modulates Wnt3A-induced osteogenic differentiation of mesenchymal stem cells via activating the PI3K/AKT/GSK3β signalling pathway. Mol Cell Endocrinol 422:243–253
19. Ni H, Chai P, Yu J, Xing Y, Wang S, Fan J et al (2020) LncRNA CANT1 suppresses retinoblastoma progression by repellinghistone methyltransferase in PI3Kγ promoter. Cell Death Dis 11(5):306
20. Pan Y, Ma S, Cao K et al (2018) Therapeutic approaches targeting cancer stem cells. J Cancer Res Ther 14(7):1469–1475
21. Wang Z, Zhao Y, Wang Y, Jin C (2019) Circular RNA circHIAT1 inhibits cell growth in hepatocellular carcinoma by regulating miR-3171/PTEN axis. Biomed Pharmacother 116:108932
22. Rong D, Sun H, Li Z, Liu S, Dong C, Fu K et al (2017) An emerging function of circRNA-miRNAs-mRNA axis in human diseases. Oncotarget 8:73271
23. Patop IL, Wüst S, Kadener S (2019) Past, present, and future of circRNAs. EMBO J 38(16):e100836
24. Kim P, Park A, Han G, Sun H, Jia P, Zhao Z (2018) TissGDB: tissue-specific gene database in cancer. Nucleic Acids Res 46(D1):D1031–D1038
25. Peter ME (2010) Targeting of mRNAs by multiple miRNAs: the next step. Oncogene 29(15):2161–2164
26. Hu J, Li L, Chen H, Zhang G, Liu H, Kong R et al (2018) MiR-361-3p regulates ERK1/2-induced EMT via DUSP2 mRNA degradation in pancreatic ductal adenocarcinoma. Cell Death Dis 9:807
27. Ogawa H, Nakashiro KI, Tokuzen N, Kuribayashi N, Goda H, Uchida D (2020) MicroRNA-361-3p is a potent therapeutic target for oral squamous cellcarcinoma. Cancer Sci 111(5):1645–1651
28. Pan L-H, Yao M, Cai Y, Gu J-J, Yang X-L, Wang L et al (2016) Oncogenic Wnt3a expression as an estimable prognostic marker for hepatocellular carcinoma. World J Gastroenterol 22:3829
29. Qi L, Sun B, Liu Z, Cheng R, Li Y, Zhao X (2014) Wnt3a expression is associated with epithelial-mesenchymal transition and promotes colon cancer progression. J Exp Clin Cancer Res 33:107
30. Zhang B, Wang Q, Pan X (2007) MicroRNAs and their regulatory roles in animals and plants. J Cell Physiol 210:279–289
31. Lyu X, Wang L, Lu J, Zhang H, Wang L (2019) microRNA-485 inhibits the malignant behaviors of retinoblastoma by directly targeting Wnt3a. Oncol Rep 41:3137–3147
32. Yang Y, Zhao Z, Hou N, Li Y, Wang X, Wu F et al (2017) MicroRNA-214 targets Wnt3a to suppress liver cancer cell proliferation. Mol Med Rep 16:6920–6927
33. Kaur N, Chettiar S, Rathod S, Rath P, Muzumdar D, Shaikh M et al (2013) Wnt3a mediated activation of Wnt/β-catenin signaling promotes tumor progression in glioblastoma. Mol Cell Neurosci 54:44–57